



The generic status of *Rattus annandalei* (Bonhote, 1903) (Rodentia, Murinae) and its evolutionary implications

MIGUEL CAMACHO-SANCHEZ,* JENNIFER A. LEONARD, YULI FITRIANA, MARIE-KA TILAK, AND PIERRE-HENRI FABRE

Conservation and Evolutionary Genetics Group, Estación Biológica de Doñana (EBD-CSIC), Avda Américo Vespucio sn, 41092 Sevilla, Spain (MCS, JAL)

Museum Zoologicum Bogoriense, Research Center for Biology, Indonesian Institute of Sciences (LIPI), Jl. Raya Jakarta-Bogor Km. 46, Cibinong 16911, Indonesia (YF)

Institut des Sciences de l'Évolution (ISEM, UMR 5554 CNRS), Université Montpellier II, Place E. Bataillon - CC 064 - 34095 Montpellier Cedex 5, France (MKT, PHF)

National Museum of Natural History, Smithsonian Institution, P.O. Box 37012, MRC 108, Washington, DC 20013-7012, USA (PHF)

* Correspondent: miguelcamachosanchez@gmail.com

The taxonomic position of Annandale's rat, *Rattus annandalei* (Bonhote, 1903), has been uncertain given its mix of *Rattus*-like and *Sundamys*-like morphological features. Annandale's rat and all described species in *Sundamys* (the lowland *S. muelleri*, and the montane *S. maxi* and *S. infraluteus*) are endemic to Sundaland, a center of diversification and endemism for their tribe, the Rattini. Using mitochondrial genomes and 3 nuclear markers (*rag1*, *rbp3*, *ghr*), we provide the 1st phylogenetic framework for *Sundamys*. We find that *R. annandalei* is nested within *Sundamys*, and that the 4 species likely diverged during the Pleistocene. We move *R. annandalei* to *Sundamys* and provide an emended diagnosis for *Sundamys*. Using geometric morphometric analyses of skulls and mandibles, we identify morphological differences between lowland and highland species of *Sundamys* that may be associated with adaptations to distinct diets.

Key words: Borneo, geometric morphometrics, mitogenomes, mountain endemics, Rattini, Sunda Shelf, *Sundamys*

Annandale's rat, *Rattus annandalei* (Bonhote, 1903), is 1 of the 5 *Rattus* species endemic to Sundaland (also: *R. tiomanicus* complex, *R. baluensis*, *R. hoogerwerfi*, and *R. korinchi*). It is a lowland species restricted to southern Peninsular Malaysia, Singapore, eastern Sumatra, and the islands of Padang and Rupa (Fig. 1). Its proper taxonomic affiliation is uncertain due to the presence of morphological characters associated with both *Rattus* and *Sundamys* (Musser and Newcomb 1983; Musser and Carleton 2005). In the 1st description of *R. annandalei*, Bonhote (1903) highlighted its large bullae, which contrasted with the small bullae in *Sundamys* (Musser and Newcomb 1983). However, a shared $2n = 42$ chromosomes (Sen 1969; Yosida 1973) and similar allozyme profiles (Chan 1977; Chan et al. 1979) pointed to a potential affinity with *Sundamys*.

Sundamys is endemic to Sundaland (Fig. 1; Musser and Newcomb 1983; IUCN 2015). It includes a widespread, lowland species, *S. muelleri*, and 2 lineages restricted to mountain ranges,

S. maxi (Java) and *S. infraluteus* (Sumatra and Borneo). The lowland *S. muelleri* inhabits all major islands of Sundaland except Java, and is sympatric with *R. annandalei* in eastern Sumatra and the southern Malay Peninsula (Musser and Newcomb 1983). *Sundamys muelleri* and *R. annandalei* occur in a variety of similar lowland habitats (Harrison and Lim 1950; Harrison 1955; Lim 1966, 1970; Muul and Liat 1971; Wilson et al. 2006). Despite being an abundant lowland species, there are occasional records of *S. muelleri* in montane forest up to 1,800 m elevation (Musser and Newcomb 1983). The mountain species *S. maxi* is only known from 21 specimens collected from 1932 to 1935 between 900 and 1,350 m from 2 mountain locations around 58 km apart, Tjiboeni (cf. Cibuni) and Mount Gede Pangrango, in western Java (Musser and Newcomb 1983). *Sundamys infraluteus* occurs in montane habitats in the north of Borneo and along several mountain ranges in Sumatra, at different elevations ranging from 700 to 2,400 m, in habitats such as lower montane oak forest and mossy forest (Musser and Newcomb 1983;

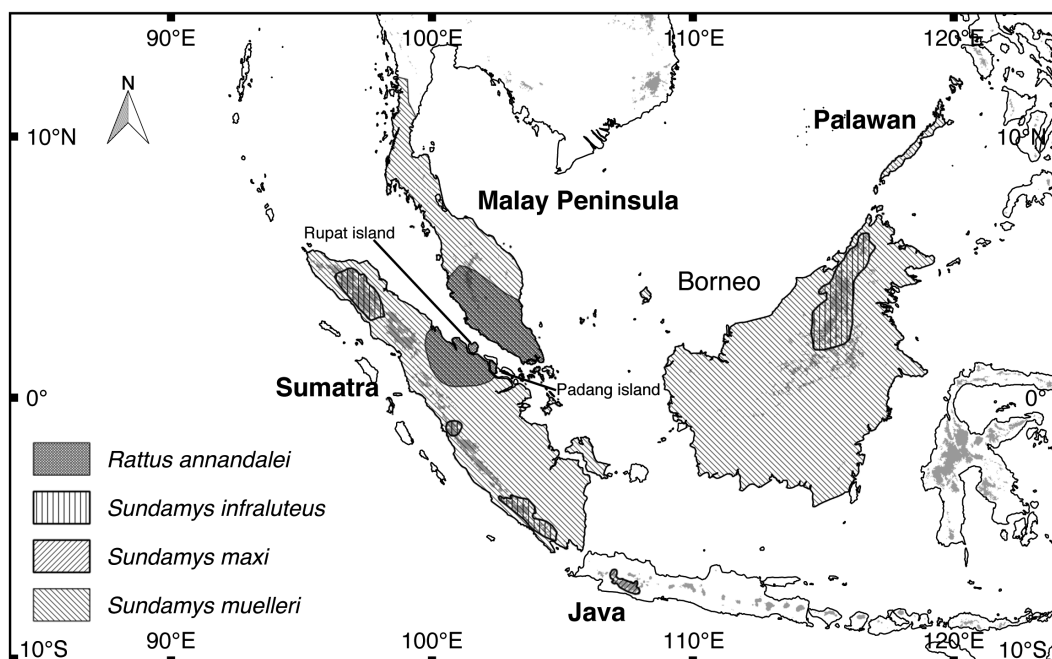


Fig. 1.—Distribution of *Rattus annandalei* and the 3 recognized species of *Sundamys*. Shaded areas indicate zones above 1,000 m elevation (data from IUCN 2015).

Musser and Carleton 2005; Cranbrook et al. 2014). Mountain habitats in Sundaland may be associated with morphological convergence in some mammals, such as has been shown with the skull of the Bornean mountain ground squirrel, *Sundasciurus everetti* (Hawkins et al. 2016) or the external morphology of Sunda highland *Rattus* (Musser 1986). The elevational distribution of the *Sundamys* species allows us to explore possible morphological divergence associated with lowland or mountain habitats.

We use protein-coding mitochondrial genes and 3 nuclear loci (*rag1*, *rpb3*, and *ghr*) to determine the relationship between *R. annandalei* and all recognized species of *Sundamys*, along with representative species of *Rattus*. We find that *R. annandalei* is phylogenetically placed within *Sundamys*, and we identify morphological characters that define this group.

MATERIALS AND METHODS

Molecular taxon and gene sampling.—We sampled a total of 27 species. Ingroup taxa included *R. annandalei* and species from the 2 genera with which it has morphological affinities: *Sundamys* and *Rattus*. In total, we included *R. annandalei*, all species in *Sundamys* (*S. infraluteus*, *S. maxi*, and *S. muelleri*), 8 Australo-Papuan and 4 Asian *Rattus* (*R. praetor*, *R. niobe*, *R. leucopus*, *R. tunneyi*, *R. villosissimus*, *R. sordidus*, *R. lutreolus*, and *R. fuscipes*; and *R. norvegicus*, *R. tanezumi*, *R. rattus*, and *R. exulans*, respectively), and other Rattini with close affinities (*Bandicota indica*, *Berymys bermorei*, *Halmaheramys bokimekot*, and *Paruromys dominator*). We also included several outgroups from the *Maxomys* division (*Maxomys surifer*), *Dacnomys* division (*Niviventer confucianus*, *Niviventer excelsior*, *Lenothrix canus*, and *Leopoldamys edwardsi*), and *Micromys* division (*Micromys minutus*). We analyzed

1 sequence per species except for the 3 *Sundamys* species and *R. annandalei*, for which we sequenced 2 individuals per species (Table 1).

When available, data were downloaded from GenBank (Table 1). Additionally, data were collected from tissue samples of historical museum specimens, modern tissue samples from animals collected in the field and vouchered (all museum acronyms in “Geometric morphometric procedures”), or from non-vouchered (NV) individuals that were sampled and released in the field. These included modern tissue of vouchered *R. annandalei* MZB 28969 and 28971 from Sumatra, tissue of historical specimens *Sundamys maxi* RMNH 21479 and 14208 from Java, modern samples of *S. muelleri* EBD 30384M and BOR448 (NV), *S. infraluteus* (field codes BOR251 and BOR510, EBD, not yet cataloged), and *L. canus* (field code BOR036, EBD, not yet cataloged; Kinabalu National Park, Malaysia); *L. edwardsi* (CBGP R4222), *B. bermorei* (CBGP L0006), and *M. surifer* (CBGP R4223; Thailand); *H. bokimekot* (MZB 33262; Halmahera); *Bunomys penitus* (field code MORT_SP, NV) and *P. dominator* (field code MORT_S46, NV; Sulawesi). Samples we collected were taken according to the guidelines of the American Society of Mammalogists (Sikes et al. 2016), and as approved by institutional animal care and use committees (Estación Biológica de Doñana Proposal Number CGL2010-21524).

We targeted mitogenomes and 3 nuclear loci previously found to be informative in murine phylogenies: *rag1* (recombination activating gene 1, exon 1); *rpb3* (retinol-binding protein 3, exon 1); and *ghr* (growth hormone receptor, exon 10—Steppan et al. 2004, 2005; Jansa et al. 2006; Lecompte et al. 2008; Rowe et al. 2008, 2011; Pagès et al. 2010; Fabre et al. 2013; Schenk et al. 2013).

Table 1.—GenBank accession numbers for sequences used for phylogenetic reconstructions. Sequences generated in this study indicated in bold. *Emended to *Sundamys annandalei* in this study.

Species	Mitochondria	<i>rbp3</i>	<i>ghr</i>	<i>rag1</i>
<i>Bandicota indica</i>	KT029807 ¹	HM217646 ²	-	-
<i>Bunomys penitus</i>	KY464167	KC878202 ³	KC878171 ³	-
<i>Halmaheramys bokimekot</i>	KY464168	KF164256 ⁴	KF164271 ⁴	-
<i>Paruromys dominator</i>	KY464169	KC953433 ⁵	EU349822 ⁶	KJ607320
<i>Rattus exulans</i>	KJ530564 ⁷	AY326105 ⁸	GQ405391 ⁹	DQ023455 ¹⁰
<i>Rattus rattus</i>	NC_012374 ¹¹	AM408328 ¹²	AM910976 ¹³	HQ334643 ¹⁴
<i>Rattus tanezumi</i>	EU273712 ¹¹	DQ191515 ¹⁵	GQ405393 ⁹	KM397346 ¹⁶
<i>Rattus norvegicus</i>	AJ428514 ¹⁷	AJ429134 ¹⁸	NC_005101 ¹⁹	AY294938 ²⁰
<i>Rattus fuscipes</i>	NC_014867 ²¹	HQ334623 ¹⁴	-	HQ334692 ¹⁴
<i>Rattus leucopus</i>	GU570659 ²¹	HQ334615 ¹⁴	EU349825 ⁶	EU349914 ⁶
<i>Rattus niobe</i>	KC152486 ²²	HQ334580 ¹⁴	-	HQ334659 ¹⁴
<i>Rattus praetor</i>	NC_012461 ¹¹	HQ334591 ¹⁴	GQ405392 ¹⁰	HQ334662 ¹⁴
<i>Rattus lutreolus</i>	GU570661 ²¹	HQ334613 ¹⁴	-	HQ334670 ¹⁴
<i>Rattus sordidus</i>	GU570665 ²¹	HQ334599 ¹⁴	-	HQ334691 ¹⁴
<i>Rattus villosissimus</i>	NC_014864 ²¹	HQ334576 ¹⁴	EU349826 ⁶	EU349915 ⁶
<i>Rattus tunneyi</i>	NC_014861 ²¹	HQ334579 ¹⁴	-	HQ334668 ¹⁵
<i>Sundamys maxi</i>				
RMNH 21479	KY464170	KY467079	KY467090	KY467070
RMNH 14208	KY464171	KY467078	KY467089	KY467071
<i>Sundamys muelleri</i>				
BOR448	KY464172	KY467080	KY467091	KY467068
EBD 30384M	KY464173	KY467081	KY467092	KY467069
<i>Sundamys infraluteus</i>				
BOR251	KY464174	KY467083	KY467088	KY467073
BOR510	KY464175	KY467077	KY467087	KY467072
<i>Rattus annandalei</i> *				
MZB 28969	KY464176	KY467082	KY467093	KY467074
MZB 28971	KY464177	KY467085	KY467086	KY467076
<i>Berylmys berdmorei</i>	KY464178	HM217639 ²		
<i>Lenothrix canus</i>	KY464180	KY467084	KY467094	KY467075
<i>Niviventer confucianus</i>	KJ152220	KC953416 ⁵	KC953293 ⁵	KC953540 ⁵
<i>Niviventer excelsior</i>	JQ927552 ²³	DQ191511 ¹⁵	GQ405386 ⁹	-
<i>Leopoldamys edwardsi</i>	KY464179	HM217688 ²	-	KJ607312
<i>Maxomys surifer</i>	KY464181	HM217682 ²	DQ019065 ¹⁰	KM397347 ¹⁶
<i>Micromys minutus</i>	KP399599 ²⁴	EU349862 ⁶	EU349818 ⁶	EU349904 ⁶

¹Wang et al. (2015), ²Pagès et al. (2010), ³Achmadi et al. (2013), ⁴Fabre et al. (2013), ⁵Schenk et al. (2013), ⁶Rowe et al. (2008), ⁷Tsangaras et al. (2014), ⁸Jansa and Weksler (2004), ⁹Heaney et al. (2009), ¹⁰Steppan et al. (2005), ¹¹Robins et al. (2008), ¹²Michaux et al. (2007), ¹³Lecompte et al. (2008), ¹⁴Rowe et al. (2011), ¹⁵Jansa et al. (2006), ¹⁶Pisano et al. (2015), ¹⁷Nilsson et al. (2003), ¹⁸Huchon et al. (2002), ¹⁹Rnor_6.0, ²⁰Steppan et al. (2004), ²¹Robins et al. (2010), ²²McComish (2012), ²³Chen et al. (2012), ²⁴Jing (2015).

DNA extraction and sequencing.—DNA was extracted using phenol-chloroform with ethanol precipitation or DNeasy Blood and Tissue Kit (Qiagen, Germantown, Maryland). Museum tissue samples from dried specimens were processed in an isolated ancient DNA laboratory. We used a modified Illumina protocol based on Maricic et al. (2010) to obtain complete mitogenomes from *R. annandalei* MZB 28969, *Sundamys* species, and *L. canus* (Supplementary Data SD1). For *B. berdmorei*, *B. penitus*, *H. bokimekot*, *P. dominator*, *R. annandalei* MZB 28971, and *M. surifer*, we obtained mitogenomes following the protocol of Tilak et al. (2015) and Fabre et al. (2016). These libraries were pooled and sequenced without enrichment as single-end reads on Illumina HiSeq 2000 lanes at the GATC-Biotech Company (Konstanz, Germany). Nuclear genes were obtained following the protocol of Fabre et al. (2014, 2016) with some modifications (Supplementary Data SD1).

Genotyping and alignment of nuclear and mitochondrial sequences.—We removed adaptors with cutadapt 1.8.3 (Martin 2011). Forward and reverse reads were paired in Geneious 8.1.5 (<http://www.geneious.com>—Kearse et al. 2012). We generated a *Sundamys* mitogenome reference by mapping reads from a modern *S. muelleri* to *Rattus norvegicus* (AJ428514) with medium–low sensitivity and 5 iterations. We used this reference to map the rest of *Sundamys* samples, *R. annandalei* (MZB 28969) and *L. canus* in Geneious. For the nuclear genes, we mapped the reads to homologous sequences from *R. norvegicus* in Geneious using medium–low sensitivity and 3 iterations. We used SAMtools 0.1.18 (Li et al. 2009) to remove PCR duplicates from the mitochondrial and nuclear BAM mapping files and called consensus sequences in Geneious (parameters: minimum 2× and 75% threshold). For other libraries, raw 101 nucleotide (nt) reads were imported into Geneious, trimmed and iteratively mapped (minimum of 24 consecutive nt perfect match to

reference, maximum 5% mismatch over read length, minimum of 3% of gaps with a maximum gap size of 3 nt) to the phylogenetically closest mitogenome available.

We used MAFFT 7.244 (Katoh et al. 2002) to align the mitogenomes. In the mitogenome alignments, we kept only protein-coding genes of the heavy strand (all genes except *nd6*) and excluded the rest. We also removed the overlapping region of *atp6* and *atp8* (43 nt), after confirming it evolves under a different evolutionary model than the sequences in the other protein-coding genes. This happens because in mitochondrial genomes the regions of adjacent genes can overlap, and thus can have stringent evolutionary constraints. The alignment was visually inspected and the genes were translated into amino acids and inspected for stop codons in Geneious.

Sequences for each nuclear gene were aligned with MAFFT using the algorithm E-INS-i to overcome alignment problems caused by low homology between some of the sequences, which could span slightly different regions in the same exon of the gene. The alignments were inspected visually and the genes were translated into amino acids and inspected for stop codons in Geneious.

We concatenated the mitochondrial and nuclear alignments into a supermatrix with the *ape* package in R (Paradis et al. 2004). This concatenated alignment was used for phylogenetic reconstructions and had 31 rows representing 27 species. For non-*Sundamys* species, the concatenated sequences were chimeric, constructed from individuals sequenced in different studies (Table 1). Each row had 15,065 nt, of which 10,798 were mitochondrial and 4,267 were nuclear. The mitochondrial alignment had 0.07% missing data, and the nuclear alignment had 36% missing data.

Phylogenetic analysis and molecular dating.—We used PhyloBayes 4.1 (Lartillot et al. 2009) for phylogenetic reconstruction based on the concatenated mitochondrial and nuclear supermatrix, as well as from each nuclear marker or mitochondrial DNA independently. PhyloBayes is a Bayesian Markov Chain Monte Carlo sampler, which incorporates methods for modeling site-specific sequence evolution variables from distributions not defined a priori, but inferred from the data. For each matrix, the CAT + GTR + Γ 4 model was selected and 2 independent chains were run for 10,000 cycles and sampled every 10 generations with a burn-in of 1,000 trees. All runs showed good convergence since the maximum difference of the bipartition frequency between both chains was < 0.1. We used a sequence from *M. minutus* to root the trees.

For comparative purposes, we computed pairwise genetic distances (proportion of nt at which 2 sequences differ) among recognized species in *Sundamys*, *R. annandalei*, and the well-studied *R. exulans* in MEGA 6.06 (Tamura et al. 2013). Distances were calculated separately for the 3 concatenated nuclear markers and for mitogenomes.

We inferred evolutionary relationships and dated divergences in a Bayesian framework with BEAST 2.4.4 (Bouckaert et al. 2014). For this purpose, we used a mitogenome matrix with only protein-coding genes and 1 sequence per species to meet the tree prior of the model. To include a calibration

point, we incorporated mitogenomes from 6 murines from 2 molecular tribes from the “*Mus*” branch of the *Rattus–Mus* split (Apodemini: *Apodemus chejuensis* HM034867, *A. latronum* NC_019585, *A. peninsulae* NC_016060; Murini: *Mus cervicolor* KJ530560, *M. cookii* KJ530561, *M. spretus* NC_025952—Fabre et al. 2013; Pagès et al. 2015). We determined the best partition scheme with PartitionFinder 2.1.1 (Lanfear et al. 2016). It splits the alignment into 3 sets corresponding to the 3 codon positions, all of which evolved under a GTR + Γ + I model, except codon position 3 of *nd6* which fell in its own partition and was discarded for downstream analysis. We split the mitogenome alignment into the former 3 partitions with AMAS (Borowiec 2016) and imported them into BEAUTi. We assigned an independent GTR + Γ + I model with estimated base frequencies and estimated substitution rate for each partition. We linked for the 3 partitions an uncorrelated relaxed clock model with rates sampled from a lognormal distribution and set a Yule model of speciation process as a tree prior. We used 11.81 million years ago (My; 95% CI: 11.11–12.68 My) as a prior for the split between the ingroup Rattini and the incorporated *Mus*-related lineages, as suggested in Kimura et al. (2015). This prior was specified in BEAST as a lognormal distribution as suggested in Morrison (2008). The *Mus–Rattus* split interval in Kimura et al. (2015) is based on a well-represented phylogeny of Murinae with nuclear and mitochondrial DNA (Fabre et al. 2013) with an extra calibration point from a new fossil of the *Mus–Arvicanthis* split. It matches the 11.0–12.3 My interval reviewed in Benton and Donoghue (2007) from *Progonomys* and *Karnimata* fossils, which has already been used for dating divergences in a mitogenome phylogeny of *Rattus* (Robins et al. 2008). Aplin et al. (2011), however, propose a more relaxed interval (i.e., 10.4–14 My) should be used to incorporate the uncertainties surrounding the fossil record of this group. We ran 2 chains in BEAST 2.4.4 on the XSEDE cluster via the Cipres Science Gateway (Miller et al. 2010) for 50 million generations, sampled every 10,000. We assessed the convergence between the 2 chains in Tracer by confirming the estimated sample size was > 200 for each of the parameters in the combined log file, after discarding the 1st 10% of generations. We discarded the 1st 10% of the trees from each chain and combined them to form the posterior. A maximum clade credibility tree was generated with TreeAnnotator.

Geometric morphometric procedures.—Photographs were taken of 122 *Sundamys* and *R. annandalei* specimens, as well as for 83 other *Rattus* specimens belonging to 9 species (*R. andamanensis*, *R. argentiventer*, *R. baluensis*, *R. exulans*, *R. losea*, *R. norvegicus*, *R. rattus*, *R. tanezumi*, and *R. tiomanicus*; Appendices I and II). We targeted a sample size of 30 adult individuals per species for *Sundamys* and 10 individuals for the *Rattus* species with an equal number of males and females. The specimens studied here are stored at the American Museum of Natural History, New York, United States (AMNH); Natural History Museum, London, United Kingdom (BMNH); Delaware Museum of Natural History, Wilmington, Delaware (DMNH); Muséum National d’Histoire Naturelle, Paris, France (MNHN); Centre de Biologie pour la Gestion des Populations, Montpellier,

France (CBGP); Estación Biológica de Doñana, Seville, Spain (EBD); Field Museum of Natural History, Chicago, Illinois (FMNH); Museum of Comparative Zoology, Harvard University, Cambridge, Massachusetts (MCZ); the Museum Zoologicum Bogoriense, Cibinong, Indonesia (MZB); Naturalis Biodiversity Center, Leiden, The Netherlands (RMNH); National Museum of Natural History, Smithsonian Institution, Washington, DC, United States (USNM); and Zoological Museum–University of Copenhagen (ZMUC). We carefully checked the skin and skull to avoid any misidentifications. All *Rattus* specimens from the CBGP were also molecularly identified (Pagès et al. 2010, 2013). Dental wear patterns were used to avoid photographing juveniles. To explore morphological variation, 25 landmarks were placed on the palatal view of the cranium for 205 specimens and 18 landmarks on the lateral view of the dentary for a subset of 95 specimens (Fig. 2). A CANON 7D video camera equipped with a macro-lens EF 100mm f/2.8L and the software TPS dig2 (Rohlf 2013) was used to obtain the photographs. We tested repeatability with 30 repetitions of landmark placement on 3 specimens of *Rattus exulans*. Measurement error was evaluated with a Procrustes analysis of variance (ANOVA) as in Claude (2013). The among- and within-specimen variances were computed based on the mean squares and cross products corresponding to the specimen and residual sources of variation. The percentage of measurement error was less than 1% for both dentary and palatal centroid size, and 8% and 6% for the palatal and dentary shape, respectively.

We used classic geometric morphometric methods (Bookstein 1991; Slice 2007; Adams and Otárola-Castillo 2013) to provide a description of the shape of the palatal view of the skull and dentary as well as to locate the most variable parts of the skull and dentary among *Sundamys* and *Rattus* species, and within *Sundamys* species. Landmark coordinates were analyzed using a general Procrustes analysis (GPA—Rohlf and Slice 1990). The logarithm of the centroid size was used as an indicator of size. A principal component analysis (PCA) was computed on superimposed coordinates (Dryden and Mardia 1998) and the scores of the principal components (PCs) were used in the multivariate analyses. We computed extreme morphologies along the 1st 2 PC axes to visualize patterns of shape variation. A 3-way linear discriminant analysis (LDA) was also computed on *Rattus* and *Sundamys* genera factors, with *R. annandalei* as an unknown factor. Thus, 3 factors were set in the LDA: *Rattus*, *Sundamys*, and *R. annandalei*. We subsequently computed the predicted values for *R. annandalei* following the protocol of Claude (2013). A multivariate analysis of covariance (MANCOVA) was run using centroid size as a covariate to test the effects of species and sex. A multivariate linear model was also applied to the PCs of shape variation using all axes with non-null eigenvalues to see the potential effect of 4 explanatory variables. The explanatory variables considered here were the minimum and maximum elevational ranges, species, size, and interactions until the 3rd order between the variables. Full-factorial multivariate analysis of variance (MANOVA) was used to test the effects of species, size, sex, and elevation (lowland versus highland) on skull and dentary shapes.

RESULTS

Sequence data.—Complete mitochondrial genomes were sequenced for 15 murines from 11 species, GenBank KY464167–KY464181. The nuclear loci (exon 10 of *ghr*, partial exon 1 of *rbp3*, and partial exon 1 of *rag1*) were sequenced for 9 animals from 5 species, GenBank KY467068–KY467094. The coverage for mitochondrial genomes ranged from 5× to 192×. Sequences for the other taxa were downloaded from GenBank (Table 1) to complete a final supermatrix with 31 samples from 27 species.

Phylogenetic results and molecular dating.—The phylogeny inferred from the mito-nuclear supermatrix was highly resolved, with a posterior probability (PP) of 1.00 for most nodes in the tree, including the clade for *Sundamys* and its internal species relationships (Fig. 3). *Rattus annandalei* is nested within *Sundamys* as the sister to *S. infraluteus* (PP = 1). The tree supports a sister relationship between *S. muelleri* and *S. maxi* (PP = 1). The genus *Berylmys* appears as sister to all other rats in the *Rattus* division included in this phylogeny. The rats from the *Dacnomys* division, *Leopoldamys*, *Niviventer*, and *Lenothrix*, form a well-supported clade sister to the *Rattus* division. A tree based on mitochondrial DNA alone was very similar to the concatenated mito-nuclear tree. However, the trees based on individual nuclear loci were not sufficiently resolved to recover well-supported relationships between *Sundamys* and other genera, or within *Sundamys* (Supplementary Data SD2).

The time to the most recent common ancestor (TMRCA) of *Sundamys* and other Rattini was estimated at 3.88 My (95% highest posterior density: 3.26–4.52 My; Fig. 4). At 2.69 My (2.16–3.18 My) *Sundamys* split into the ancestors of *S. muelleri* + *S. maxi* and *R. annandalei* + *S. infraluteus*. The split between *S. infraluteus* and *R. annandalei* was estimated at 2.22 My (1.74–2.71 My), whereas the split between *S. maxi* and *S. muelleri* was more recent: 1.22 My (0.90–1.57 My).

The mitochondrial and nuclear distances between *R. annandalei* and any species of *Sundamys* were 1) smaller than between it and a supposed *Rattus* congener, and 2) within the range of distances among recognized *Sundamys* species (Table 2). Mitochondrial distances were approximately an order of magnitude greater than nuclear distances.

Morphometric results from *Sundamys*–*Rattus* comparisons.—Palatal analyses of *Rattus* and *Sundamys* species clearly illustrate the mixed features of *R. annandalei* (Fig. 5A). PC1 and PC2, respectively, explained 45.3% and 8.3% of the variance (eigenvalues and landmark loadings in Supplementary Data SD3 and SD4). PC1 separated *Rattus* from *Sundamys*. *Rattus* species tend to have a shorter rostrum, longer incisive foramina, longer palatal bridge, wider bullae tympanica, narrower incisors, shorter molar rows, a wider braincase, and a longer basicranium (Fig. 5A; see variation on PC1, black line). *Sundamys* species tend to have a longer rostrum, shorter bullae tympanica with a well-defined Eustachian tube, wide incisors, a narrow skull, and a shorter braincase (Fig. 5A). The morphospace of *R. annandalei* falls between those of *Rattus* and *Sundamys*, a pattern fully detailed in the following emended diagnosis. A 3-way LDA was subsequently

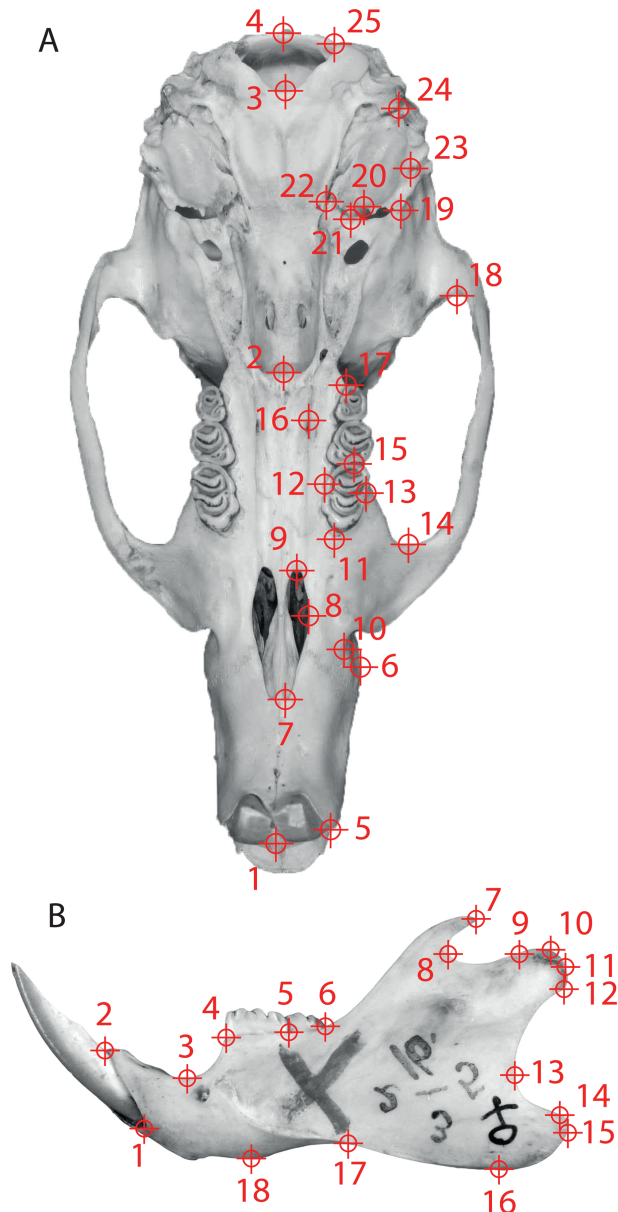


Fig. 2.—Landmark locations and definitions on the palatine and dentary views of the *Sundamys* and *Rattus* specimens. A) palatine side: 1) premaxillary bone between anterior margin of upper incisors, 2) posterior margin of the palatal bone, 3) anterior margin of the foramen magnum, 4) posterior margin of the foramen magnum, 5) lateral margin of the right incisor, 6) lateral marginal of the lacrymal notch, 7) anterior margin of the incisive foramina, 8) lateral margin of the incisive foramina, 9) posterior margin of the incisive foramina, 10) maxillary insertion of the zygomatic root, 11) anterior margin of the 1st upper molar, 12) lingual margin of M1 at the level of the 2nd lamina, 13) labial margin of M1 at the level of the 2nd lamina, 14) anterior margin of the orbit, 15) posterior margin of M1, 16) posterior margin of the posterior palatine foramina, 17) posterolateral margin of M3, 18) posterior margin of the temporal fossa, 19) suture between squamosal and sphenoid, 20) junction between bulla tympanica and eustachian tube, 21) lateral tip of the eustachian tube, 22) junction between basioccipital and basisphenoid, 23) most internal point of the external auditory meatus, 24) contact between bulla tympanica and jugular process, 25) lateral margin of the foramen magnum. B) Dentary lateral side: 1) ventral margin of mandible at insertion of incisor, 2) dorsal

margin of mandible at insertion of incisor, 3) lowest point on dorsal surface of mandible between incisor and m1, 4) anterior margin of m1 at insertion, 5) insertion of m2 at posterior margin, 6) intersection of the ascending branch of the mandible and the molar row, 7) dorsal-most point of the coronoid process, 8) deepest point of condylar neck, 9) anterior-most point of the articular condyle, 10) dorsal-most point of the articular condyle, 11) posterior-most point of the articular condyle, 12) ventral-most point of the articular condyle, 13) anterior-most point between articular condyle and angular process, 14) dorsal-most point of the angular process, 15) posterior-most point of the angular process, 16) ventral-most point of the angular process, 17) dorsal-most point on the ventral margin of mandible anterior to angular process, 18) ventral-most part of the mandible anterior to 17.

computed to estimate the predicted morphological attribution of *R. annandalei*. Once again *R. annandalei* fell in a singular morphospace with intermediate values between *Sundamys* and *Rattus* for the LD1 axis (leave-one-out cross-validation on LD1, CV1 = 31.9%), that best discriminates *Rattus* and *Sundamys*, and LD2 (CV2 = 12.6%) which isolates *R. annandalei* from the other discriminant factors (*Rattus* and *Sundamys*; Fig. 5B). Taking *R. annandalei* as an unknown factor, 14 specimens were attributed to *Rattus* and 19 specimens to *Sundamys*.

Morphometrics of the *Sundamys* cranium.—PC1 and PC2, respectively, explained 38.4% and 9.0% of the variance (Fig. 6A). The 1st PC discriminates *R. annandalei*, in the negative region of PC1 and *S. infraluteus*, in the positive region, whereas *S. maxi* and *S. muelleri* occupy central positions, with *S. maxi* closer to *S. infraluteus*. This axis is correlated with smaller braincase, smaller tympanic bullae with a small Eustachian tube, and a small 1st upper molar (Fig. 6A; Supplementary Data SD5 and SD6 for eigenvalues and loadings). A MANOVA computed on the PC scores revealed a highly significant effect of species ($F_{3,33} = 30.9$, $P < 0.0001$), elevation ($F_{1,11} = 128.2$, $P < 0.0001$), and size ($F_{1,11} = 39.8$, $P < 0.0001$), but no effect of sex ($F_{2,22} = 1.5$, $P = 0.07$). No significant interaction ($P = 0.20$) was detected between species and size ($F_{2,22} = 1.28$, $P < 0.02$) or between elevation and size ($F_{1,11} = 1.4$, $P = 0.19$). A MANCOVA performed on centroid size indicated significant effects of species ($F_{3,1} = 17.4$, $P < 0.0001$) and elevation ($F_{1,1} = 38.6$, $P < 0.0001$).

Morphometrics of the *Sundamys* mandible.—PC1 and PC2 represented 32.3% and 16.1% of the explained variance, respectively (Fig. 6B; Supplementary Data SD7). These axes are less discriminating compared to the palatal view of the skull. PC1 separated the dentary of lowland species (*R. annandalei* and *S. muelleri*) and highland species (*S. infraluteus* and *S. maxi*; loadings in Supplementary Data SD8). The dentary of the highland species is more dorsoventrally compact. In highland *Sundamys*, the angular process is shorter and does not extend ventroposteriorly to the articular process. The m1 as well as the molar row is also longer in these highland species. PC2 is mainly correlated with the age of the specimen and size. The coronoid process of the highland species is shorter and situated closer to the large condyloid process (Figs. 6B and 7). A MANOVA computed on the PC scores revealed highly significant effects of species ($F_{3,24} = 8.70$, $P < 0.0001$) and size ($F_{1,8} = 11.4$, $P < 0.0001$), nonsignificant interaction between

margin of mandible at insertion of incisor, 3) lowest point on dorsal surface of mandible between incisor and m1, 4) anterior margin of m1 at insertion, 5) insertion of m2 at posterior margin, 6) intersection of the ascending branch of the mandible and the molar row, 7) dorsal-most point of the coronoid process, 8) deepest point of condylar neck, 9) anterior-most point of the articular condyle, 10) dorsal-most point of the articular condyle, 11) posterior-most point of the articular condyle, 12) ventral-most point of the articular condyle, 13) anterior-most point between articular condyle and angular process, 14) dorsal-most point of the angular process, 15) posterior-most point of the angular process, 16) ventral-most point of the angular process, 17) dorsal-most point on the ventral margin of mandible anterior to angular process, 18) ventral-most part of the mandible anterior to 17.

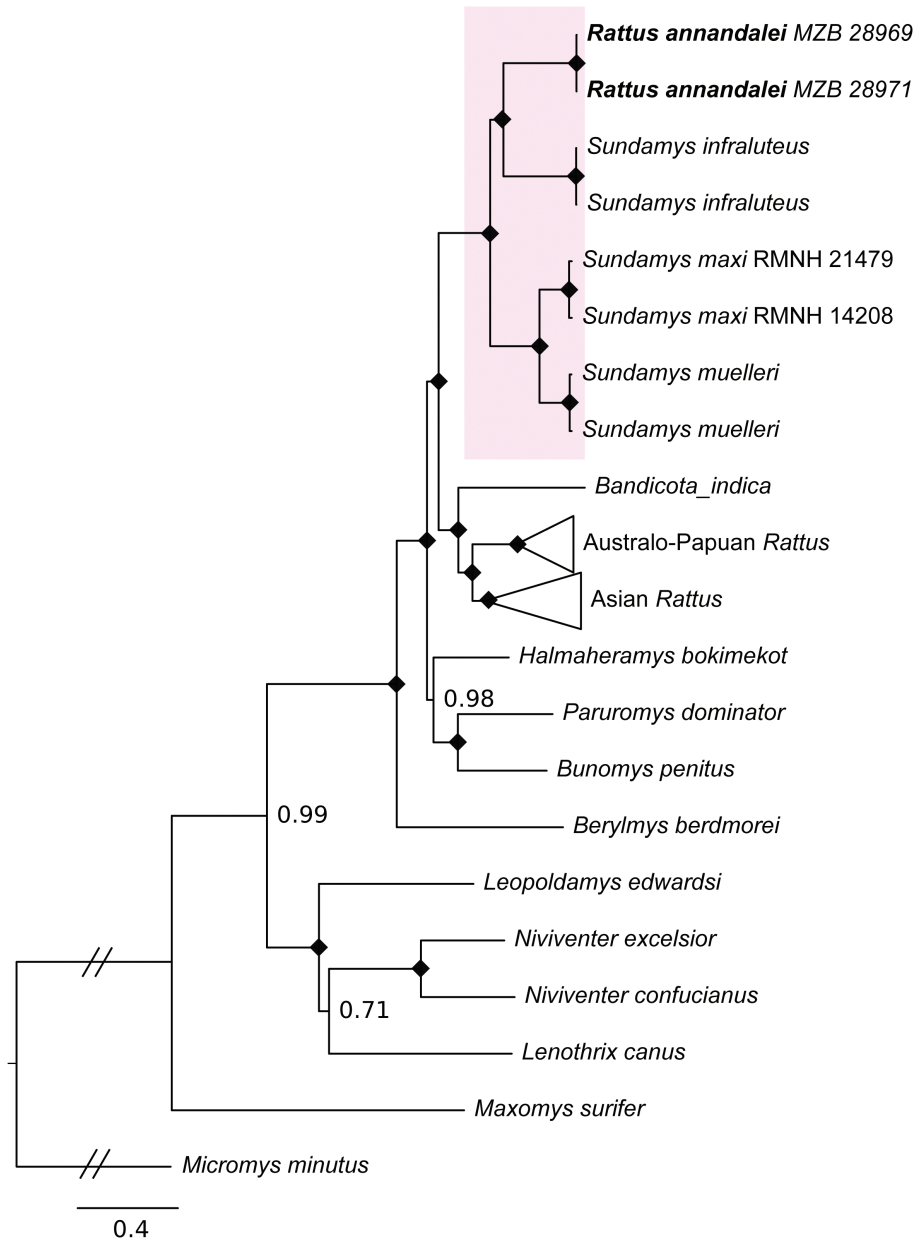


Fig. 3.—PhyloBayes maximum clade credibility tree for the concatenated mitochondrial protein-coding genes on the heavy strand (10,798 bp) and nuclear loci (*rbp3*, *ghr*, and *rag1*, 4,267 bp). Posterior probabilities (PPs) are indicated by diamonds when PP = 1.00, otherwise with a number.

species and size ($F_{3,24} = 1.3$, $P = 0.22$), and nonsignificant effect of sex ($F_{2,16} = 0.61$, $P = 0.76$). A MANCOVA computed on centroid size show highly significant effects of species ($F_{2,1} = 22.99$, $P < 0.0001$) and elevation ($F_{1,1} = 21.99$, $P < 0.0001$).

Sundamys Musser and Newcomb, 1983

Type species.—*Mus mülleri* Jentink, 1879.

Phylogeny.—*Sundamys* belongs to the *Rattus* division of the Rattini tribe in the Murinae subfamily. It is closely related to the widespread genus *Rattus*; the Philippine genus *Bullimus*; Sulawesi genera *Bunomys*, *Paruromys*, and *Taeromys*; and the Moluccan genus *Halmaheramys* (see also Fabre et al. 2013).

Emended diagnosis.—Once considered part of *Rattus*, *Sundamys* was defined by Musser and Newcomb (1983) to include 3 species: *S. muelleri*, *S. infraluteus*, and *S. maxi*. Our molecular phylogenies clearly support the inclusion of *R. annandalei* within *Sundamys*. Based on this new result, we provide an emended diagnosis of *Sundamys*.

Sundamys species are characterized by the following: 1) medium to large body size (body mass range: 150–643 g; Table 3) compared to other Rattini from the Sundaic region (e.g., *Niviventer*, *Maxomys*); 2) a slightly inflated rostrum without a marked constriction anterior to the lacrymal notch; 3) 4 pairs of mammae (1 pectoral + 1 post-axillary + 2 inguinal) in all species except *S. infraluteus* (1 post-axillary + 2 inguinal); 4) incisive foramina are short relative to

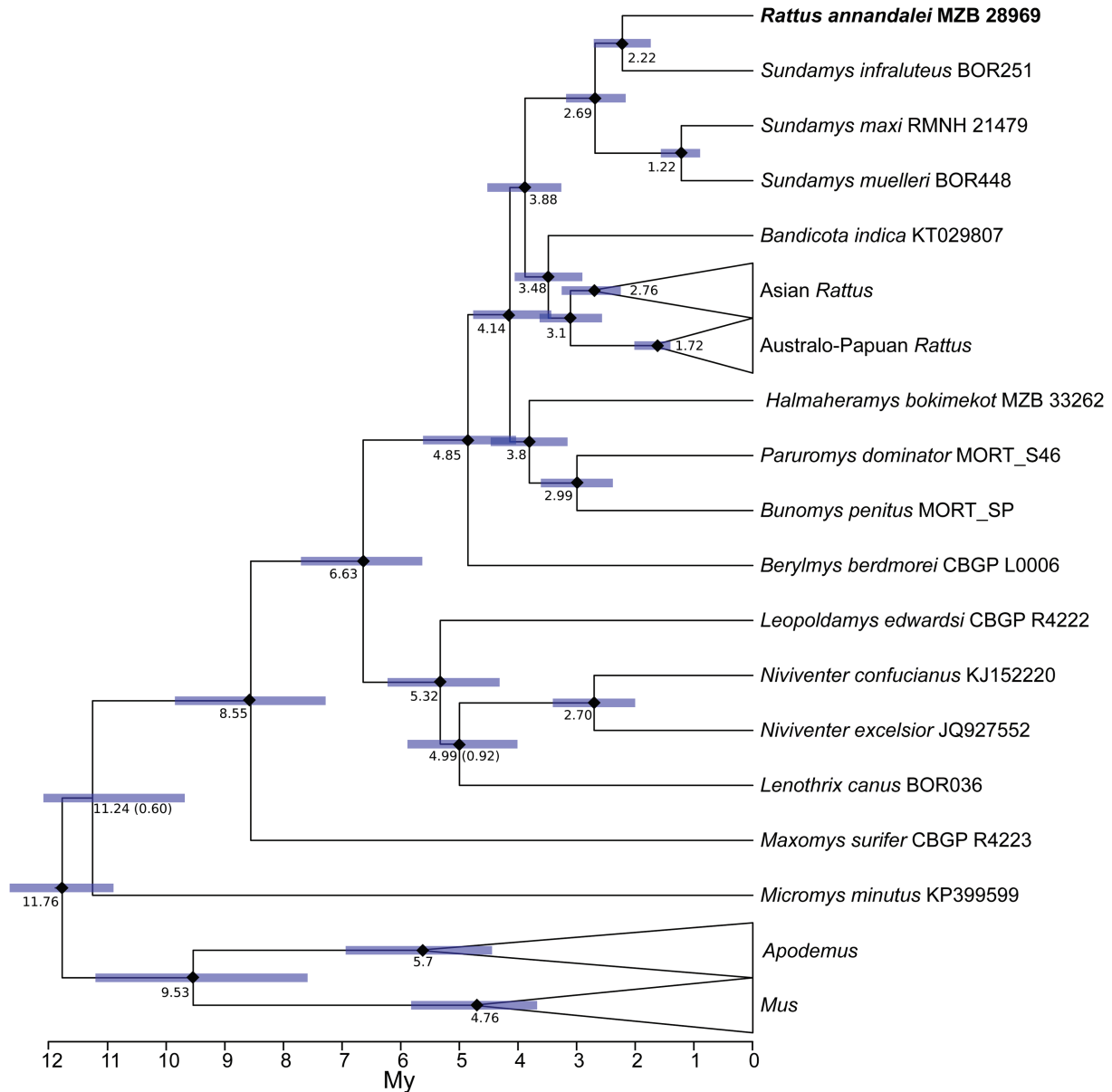


Fig. 4.—Maximum clade credibility tree from BEAST analysis of the protein-coding genes on the heavy strand of the mitochondria. Node bars indicate 95% highest posterior density in divergence times. Numbers on nodes represent ages in million years ago (My). Posterior probabilities equal to 1.00 are indicated with diamonds on the nodes, or otherwise with a number in parentheses.

Table 2.—Uncorrected pairwise genetic distances (p) between *Rattus annandalei*, all *Sundamys* species, and a *Rattus* species with a well-defined taxonomy, *Rattus exulans*, for mitogenomes (upper triangular) and concatenated nuclear markers *rbp3*, *rag1*, and *ghr* (lower triangular).

	1	2	3	4	5
1. <i>Rattus annandalei</i>		0.095	0.102	0.101	0.120
2. <i>Sundamys infraluteus</i>	0.012		0.101	0.098	0.116
3. <i>Sundamys maxi</i>	0.012	0.013		0.062	0.119
4. <i>Sundamys muelleri</i>	0.010	0.014	0.005		0.118
5. <i>Rattus exulans</i>	0.022	0.021	0.025	0.023	

condylobasal length and usually do not reach anterior margin of M1 (Fig. 7); 5) small sphenopalatine vacuity; 6) upper molars are anchored by 5 (M1), 4 (M2), or 3 roots (M3);

7) lower molars are anchored by 4 (m1) or 3 roots (m2, m3); 8) palatal bridge extends only slightly beyond the molar rows without forming a wide and deep shelf (Fig. 7); 9) mesopterygoid fossa is wide and connects with the sphenopalatine vacuity; 10) the posterior cingulum is often present on M1; 11) M2 and M3 usually have large and well-developed cusp t3 (sensu Musser 1981; Musser and Newcomb 1983); 12) lower molars have wide lamina made of similar size cusps that do not form lamina with arcuate or acute angles; 13) anterolabial and anterolingual cusps of m1 are fused and form a large lamina; 14) the antero- and posterolabial cusplets on m2 are always present and well developed.

Content and distribution.—*Sundamys* includes 4 species confined to the Sunda Shelf region: *Sundamys annandalei*, *S. infraluteus*, *S. maxi*, and *S. muelleri*.

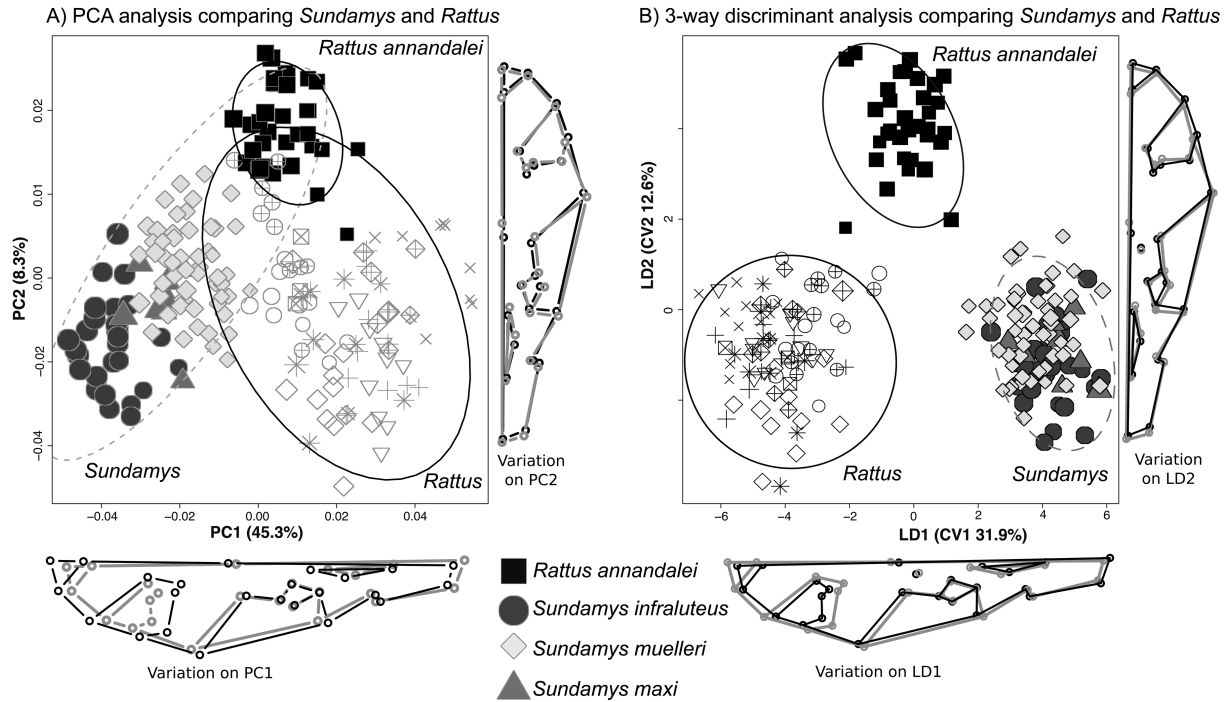


Fig. 5.—A) Principal component and B) 3-way discriminant analyses of morphological variation for the cranium (palatal view) among *Sundamys* and Indo-Pacific *Rattus* species. Patterns of shape variation along PC1 and PC2 (A) and LD1 and LD2 (B) are illustrated on the right and below each graph. Light gray lines and circles correspond to minimal scores, and black lines and circles to maximal values. Symbols are proportional to centroid skull and dentary size. Open symbols correspond to *Rattus* species and closed symbols to *Sundamys*. Ellipses show 95% confidence area for each genus and *R. annandalei*. List of *Rattus* and *Sundamys* species as well as their voucher numbers are indicated in [Appendix I](#).

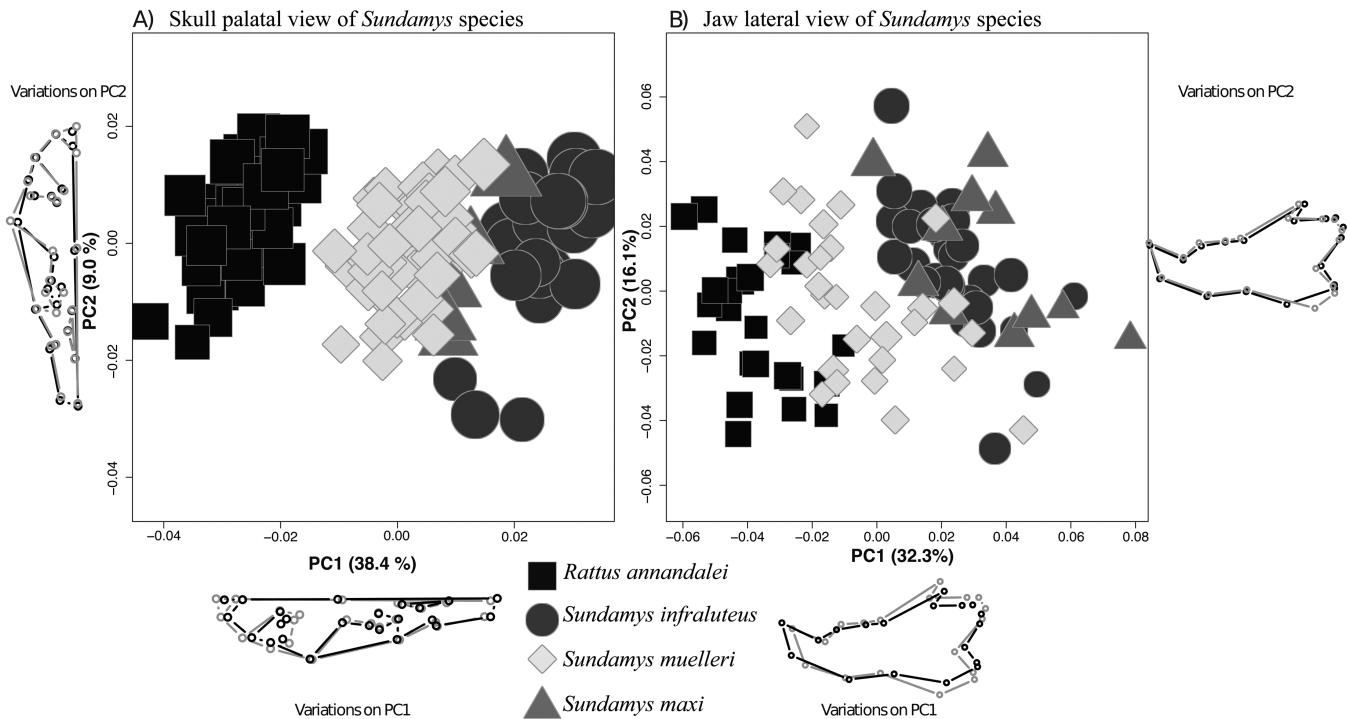


Fig. 6.—Principal component analysis for the palatal view of the cranium (A) and lateral view of the mandible (B) among *Sundamys* species and *Rattus annandalei*. Patterns of shape variation along PC1 and PC2 are illustrated on the side and below each graph, with light gray lines and circles corresponding to minimal scores, black lines and circles corresponding to the maximal scores. Symbols are proportional to centroid skull and dentary size. List of *Sundamys* species as well as their voucher numbers are indicated in [Appendices I and II](#).

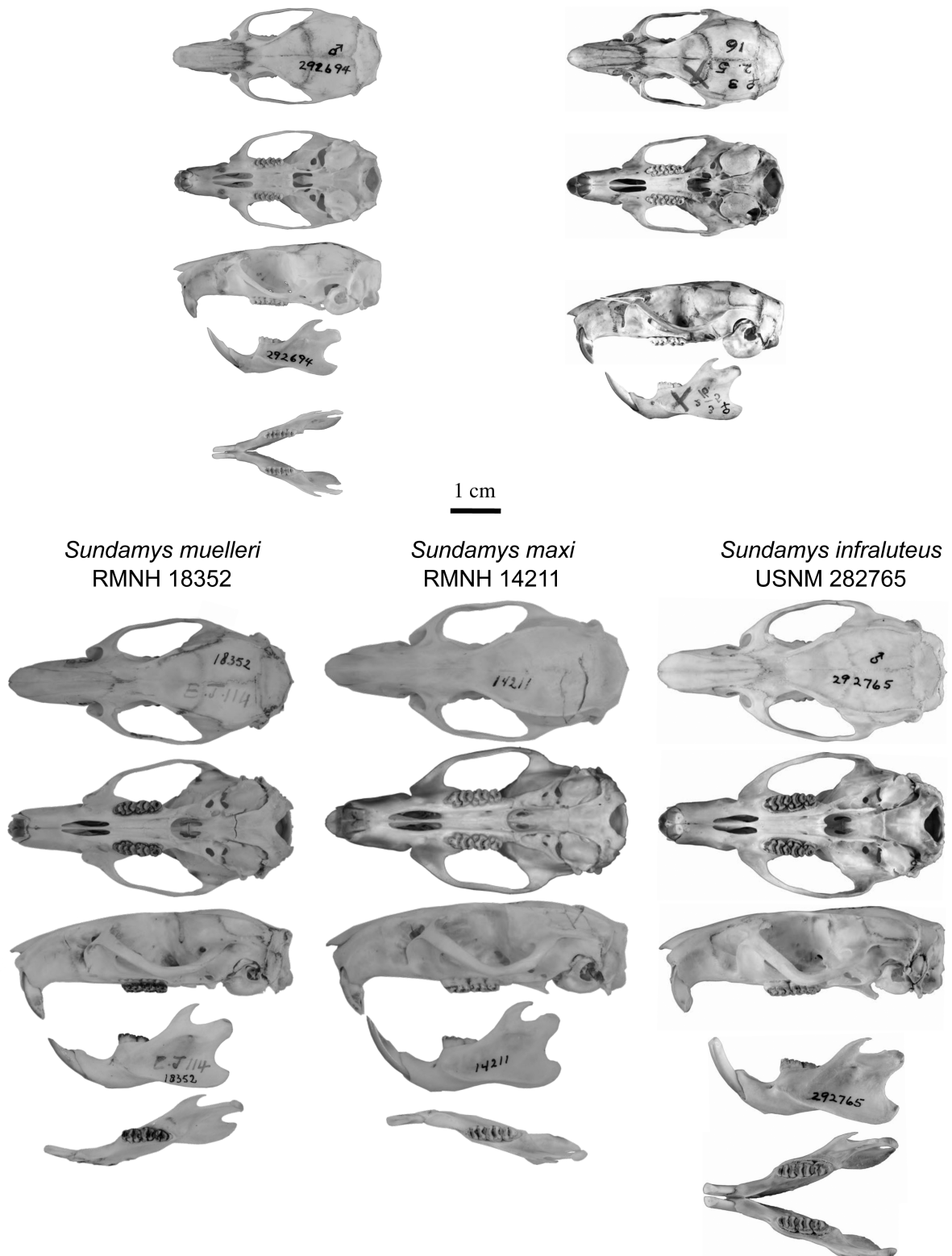
Rattus baluensis USNM 292694*Rattus annandalei* BMNH 1903.2.5.16

Fig. 7.—Dorsal, palatal, and lateral views of the skull, plus lateral and occlusal views of the dentary of *Rattus baluensis*, *Sundamys annandalei*, and the 3 previously recognized *Sundamys* species (*S. muelleri*, *S. maxi*, and *S. infraluteus*).

Sundamys annandalei (Bonhote, 1903).

Mus annandalei Bonhote, 1903:30. Type locality. Malaysia (Malay Peninsula), South Perak, Sungkei.

Mus bullatus Lyon, 1908:646. Type locality Pulo Rupert, off east coast of Sumatra.

Mus villosus Kloss, 1908:146. Type locality Singapore Island.

Emended comparison with other Sundamys species.—*Sundamys annandalei* is smaller (head-body range: 173–220 mm; body mass range: 150–261 g) than other *Sundamys* (head-body range: 185–299 mm; body mass range: 196–643 g; Table 3). Its dorsum is grayish brown and its belly ranges from white to pale yellow, grayish white or buff white. It is very similar in color pattern to *S. muelleri*, although the taxa differ in body size and proportions. Indeed, *S. muelleri* is a larger species and can be twice the weight of *S. annandalei*. The fur of *S. annandalei* is shaggy, and soft, with some longer guard hairs present on the rump. Compared to *S. annandalei*, both *S. maxi* and *S. infraluteus* are giant rats with dull, soft, dark fur on the dorsum and paler on the belly. Tail length is longer than head-body length in all *Sundamys* species. One major difference among *Sundamys* species is the foot length, which is shortest in *S. annandalei* (37–41 mm) and largest in *S. infraluteus* (55–61 mm; Table 3). *Sundamys annandalei* has the following mammae formula: 1 pectoral + 1 post-axillary + 2 inguinal, with a total of 8 teats.

Similar to overall body size, the skulls of *S. maxi* and *S. infraluteus* are much larger than those of *S. annandalei* and *S. muelleri* (Fig. 7). Dorsally, the skull of all *Sundamys* are very similar in proportion apart from the ridging of the supra-orbital and temporal regions, which is more marked in the larger *S. infraluteus* and *S. maxi*, likely due to larger temporalis muscle in these species. With the exception of *S. maxi*, all *Sundamys* species have the common murid arterial pattern (following Musser and Newcomb 1983) with the stapedia artery branching into the tympanic bulla and branching laterally to

become the internal maxillary artery. In *S. maxi*, this branch is reduced or absent, and the internal maxillary artery is branching from the main internal carotid artery. The position of the transverse canal is generally anterior to the posterior opening of the alisphenoid canal.

In palatal view, most *Sundamys* species have the zygomatic plate of the zygomatic arch placed anterior to M1. However, in *S. infraluteus*, the zygomatic plate overlaps with M1 along the anteroposterior axis. In *S. annandalei*, the squamosal root of the zygomatic arch is near the tympanic bullae. Other *Sundamys* species have reduced tympanic bullae not overlapping with the squamosal root of the zygomatic arch along the anteroposterior axis. In palatal and lateral view, the major distinction of *S. annandalei* compared to other *Sundamys* species is its large and inflated tympanic bullae. The tympanic bulla is smaller in all other species of *Sundamys*. Except for some individuals of *S. maxi*, an alisphenoid strut is present in most specimens. In *S. annandalei* and *S. maxi*, the sphenopterygoid vacuity is present, being much larger in most specimens of *S. maxi* (see Musser and Newcomb 1983:467). In the other species, this vacuity is closed with a bony wall. Except for some *S. infraluteus* specimens, the sphenoid and vomer bridge is always present and well visible between the mesopterygoid fossa.

Concerning molar teeth, most *Sundamys* species have 5 roots under the M1, 4 roots under M2, and 3 roots under M3. It is only in *S. muelleri* that some specimens were found to have either 3 or 4 roots on M3. On the lower molars, we observed no variation, with 4 roots under m1 and 3 roots under m2 and m3. Compared to the skull length, the molars are small in both *S. annandalei* and *S. muelleri*. Another state is found in *S. infraluteus* and *S. maxi* where both species have large molars relative to skull length. However, despite this large molar size, the cusp pattern of *S. maxi* is more similar to that of *S. muelleri* (Musser and Newcomb 1983). On the M1, a posterior cingulum is present in all *Sundamys* species. On M2 and M3, the cusp t3 is present and well developed in most of the observed specimens

Table 3.—Selected external measurements (mm) and body mass (g) of adult *Sundamys* species from the main landmasses. Mean, sample size (in parenthesis), and range (in brackets) are reported in each case.

	<i>Sundamys muelleri</i>			<i>Sundamys infraluteus</i>		<i>Sundamys maxi</i>	<i>Sundamys annandalei</i>	
	Malay Peninsula	Sumatra	Sabah	Sabah	Sumatra	Java	Malay Peninsula	Sumatra
Head-body (HB)	243.1 (58) [209–299] ¹	207.3 (23) [185–236] ¹	207.7 (22) [188–240] ¹	258.5 (10) [229–282] ¹	266 (3) [259–276] ¹	241.5 (8) [218–270] ¹	191.8 (24) [173–220] ¹	192
Tail (TL)	285.6 (58) [248–370] ¹	260.6 (22) [214–301] ¹	247.4 (22) [212–271] ¹	315.8 (10) [289–343] ¹	311.7 (3) [298–333] ¹	286.7 (7) [258–309] ¹	240.2 (24) [225–263] ¹	227
Hindfoot	51.5 (62) [47–55] ¹	45.3 (23) [42–49] ¹	40.9 (22) [37–45] ¹	57.5 (11) [55–61] ¹	58.7 (3) [57–60] ¹	53.1 (7) [52–55] ¹	39.5 (24) [37–41] ¹	38.94
Ear	23.2 (57) [20–27] ¹	21.4 (23) [20–23] ¹	21.4 (7) [21–23] ²	24.8 (10) [22–27] ¹	25.7 (3) [24–29] ¹	25.4 (7) [24–28] ¹	21.2 (24) [20–23] ¹	21.31
TL/HB	116 ¹	121 ¹	119 ¹	122 ¹	117 ¹	119 ¹	125	118
Body mass	335.4 (30 ♂) 292.4 (30 ♀) ³	NA	262 (8 ♂) 196 (3 ♀) ²	468 (2 ♂) 550 (2 ♀) ²	582 (2) [521–643] ¹	NA	197.4 (15) [155–261] ^{1,4}	150

¹Musser and Newcomb (1983:428, 442, 452, 502) (claws included in hindfoot measurement).

²Field measurements.

³Lim (1970).

⁴MNHN and USNM.

of *S. muelleri*, *S. maxi*, and *S. annandalei*. Concerning the lower cheek teeth, *S. annandalei* and all other species of *Sundamys* lack a posterior cingulum on m3 and they all have a posterolabial cusplet on m1. Anterolabial cusplet on m1 is often absent (in 70% of the observed specimens). Antero- and posterolabial cusplets are usually present on m2 in all *Sundamys* species. The same is true for the posterolabial cusplets on m3.

The dentary distinguishes high-elevation *Sundamys* species from the low-elevation ones. As discussed in our morphometric results, both lowland *S. muelleri* and *S. annandalei* have proportionally less elongated dentary compared to highland *S. infraluteus* and *S. maxi* ones (Fig. 6B). The angular process of *S. annandalei* and *S. muelleri* is wider and more posterior-ventrally elongated as compared to *S. infraluteus* and *S. maxi*, only slightly extending posteriorly beyond the condyloid process (Fig. 6B). Another clear-cut difference is the length of the lower molar row, which is longer in the highland *S. infraluteus* and *S. maxi*. The rami are also shorter in the highland *S. infraluteus* and *S. maxi*. The higher coronoid along with robust dentary (with a short and wide angular) constitute a more powerful in-lever arm for gnawing with high mechanical advantage for these lowland species. Further, the wide and robust angular configuration indicates a larger insertion for the superficial masseter, which reinforces their dentary lever advantage at the incisor.

Nomenclatural statement.—A life number was obtained for the new name combination *Sundamys annandalei*: urn:lsid:zoobank.org:pub:D6AA5C4F-6A6A-4CEF-B326-29C3485A82CC.

DISCUSSION

Taxonomic status of *Sundamys annandalei*.—Based on our molecular phylogenies inferred from nuclear and mitochondrial DNA and the morphological data, we reclassify *R. annandalei* as *S. annandalei*. This taxonomic change is supported by the previous morphological revision of this species (Musser and Newcomb 1983) and our emended diagnosis of *Sundamys*. It resolves a longstanding debate on the taxonomic status of this taxon. Symplesiomorphies in the skull and dentition caused the confusion surrounding *S. annandalei* and also hinder the taxonomy of other Indo-Australian murids (Musser and Newcomb 1983). Several species will likely be revised in the near future (see also Musser and Carleton 2005), such as the extinct *Rattus macleari* and *R. nativitatis* from the Christmas Islands, or the Flores and Timor rats (*R. timorensis* and *R. hainaldi*—Musser and Newcomb 1983). Museums are a key resource for better understanding the evolution and diversity of the Rattini, since some of the lineages are already extinct (*R. macleari*, *R. nativitatis*), have an unknown conservation status (*S. maxi*), or have only been recorded by a handful of specimens in museums (e.g., *R. blangorum*, *R. korinchi*, and *Pithecheirops otion*). Further molecular studies are required to test for the monophyly of *Rattus* and to more accurately define taxonomic groups within the Indo-Pacific region (Rowe et al. 2011; Fabre et al. 2013).

***Sundamys* biogeography and ecology.**—Our nuclear and mitochondrial analyses indicate close affinities between *Sundamys*

and the genera *Rattus*, *Paruromys*, *Bunomys*, *Halmaheramys*, and *Bandicota*, as also identified in the most recent studies of these groups (Fabre et al. 2013; Schenk et al. 2013). Assuming our date estimates are reasonably accurate, the *Sundamys* lineage diverged from other Rattini in the Pliocene, ~2.69–3.88 My. Other studies on Indo-Pacific murids find that many of the genera in Rattini originated during the Late Pliocene, following range expansions to new archipelagos (i.e., Sahul, Philippines, Wallacea, and Sundaland), whereas most of the intrageneric diversification has occurred within archipelagos during Late Pliocene and Pleistocene (Fabre et al. 2013; Schenk et al. 2013). This is coherent with a dynamic mosaic of intermittent physical (sea-level) and ecological (drier vegetation during glacial periods) barriers during the Plio–Pleistocene, which seem to have shaped much of the diversification of forest mammals in Sundaland (Ruedi and Fumagalli 1996; Esselstyn et al. 2013; Leonard et al. 2015; Demos et al. 2016). A Pleistocene origin is suggested for *S. infraluteus* (~2.22 My) and other Sunda mountain small mammals, such as *Rattus baluensis* (Aplin et al. 2011) or mountain shrews in Java and Sumatra (Esselstyn et al. 2013; Demos et al. 2016), but contrasts with the pre-Pleistocene origin of highland lineages in Sunda squirrels (den Tex et al. 2010; Hawkins et al. 2016) and treeshrews (Roberts et al. 2011). Whereas all of these date estimates are crude, we need more nuclear markers and a wider sampling across the Sunda shelf to assess the effects of Late Pliocene–Pleistocene changes within and between species of *Sundamys*.

Sundamys muelleri and *S. annandalei* are sympatric across the entire distribution of *S. annandalei* (eastern Sumatra and southern Peninsular Malaysia; Fig. 1). These 2 species have been trapped in the same surveys (Rudd 1965; Shariff 1990), but it is unclear whether they occur in syntopy. Both can be found in forests and seem to have a preference for the same altered habitats (Lim 1966, 1970; Muul and Liat 1971; Wilson et al. 2006; Wells et al. 2007). Nevertheless, *S. annandalei* is smaller and apparently more arboreal than *S. muelleri*, which is a ground species (although there are some records on trees) often associated with wetter habitats, such as riparian areas (Harrison and Lim 1950; Harrison 1955; Lim 1966, 1970; Muul and Liat 1971). Despite the lack of fine-scale data on the possible syntopy of these 2 species, the differences in ecology, together with morphological divergence in the skull (Fig. 6) and external morphology (Table 3), suggest different niches for *S. annandalei* and *S. muelleri*. However, it is not clear under what ecological conditions *S. annandalei* might have originated, and why it has such a restricted distribution given that there are no apparent ecological barriers to limit its expansion across Sumatra and Peninsular Malaysia.

Morphological divergence in *Sundamys*.—Our morphometric analyses show that lowland and highland taxa occupy different parts of the morphospace for their skull and dentary (Fig. 6). The lowland *S. muelleri* and *S. annandalei* have larger braincases, larger bullae, and a shorter and broader dentary compared to their highland counterparts (*S. maxi* and *S. infraluteus*). This divergent morphology of the dentary could reflect dietary adaptations, as has previously been found

in other Murinae (Satoh 1997; Michaux et al. 2007). Muscle insertions and dentary morphology suggest a higher gnawing capacity (able to process harder food) in both lowland species, *S. annandalei* and *S. muelleri*. On the other side, highland species with a short in-lever (short condylo-angular distance) and both long molar row and slender jaw (resulting in long out-lever) are likely to be able to close jaws faster, but have less powerful gnawing and chewing capacities. However, the greater molar size provides more chewing surface to process food material in the highland species and this might compensate for this mechanical disadvantage.

Wider and elongated angular processes and shorter molar rows, as in the lowland *Sundamys*, have been shown to have a role in gnawing capacities and reduced chewing capacities in some omnivorous rodents (Satoh 1997; Renaud et al. 2007; Samuels 2009) and some herbivorous lineages (*Hapalomys*, *Chiropodomys*, *Pogonomys*, and *Chiruromys*). In some other cases, a larger braincase might be associated with arboreality or to more developed sensory and perceptual capacities, and may indicate the presence of more complex foraging behaviors and more carnivorous or omnivorous diets as compared to folivorous diets (Harvey et al. 1980; Mace et al. 1981). Also, an inflated bullae could be an adaptation to predatory avoidance in lowland *Sundamys*, as has been shown in other rodent communities (Kotler and Brown 1988). More ecological, morphological, and genomic data are needed to better understand the potential roles of divergence and convergence in the evolutionary history of lowland and highland *Sundamys*.

ACKNOWLEDGMENTS

We thank M. Lakim, F. Tuh, Y. Yuh (Sabah Parks, Sabah, Malaysia), M. Hawkins, L. R. Hawkins, F. P. Peter, M. L. Rivera, F. A. C. Marino, and the Malayan porters and field assistants that participated in fieldwork. We thank 2 anonymous referees for discussions or corrections concerning this manuscript. We are grateful to the following people and institutions for granting access to specimens: P. Jenkins, S. Oxford, K. Dixey, and R. P. Miguez (NHM); D. Lunde, N. Edmison, and K. Helgen (NMNH, Smithsonian Institution); E. Westwig, N. Duncan, and R. Voss (AMNH); H. Baagøe and M. Andersen (ZMUC); G. Véron, V. Nicolas, and C. Denis (MNHN); S. van Der Mije (NBC); J. Woods (DMNH); J. Chupasko (MCZ); Y. Chaval, S. Morand, and J. Claude (CBGP); and the Doñana Biological Station (EBD). S. Y. W. Ho provided valuable insight regarding molecular dating. We are grateful to F. Catzeflis for his comments and access to the Montpellier mammal skeleton and tissue collection. We thank A. Mortelliti and R. Castiglia for granting access to tissue of *Paruromys* and *Bunomys*. We thank the team of the CERoPath project (www.ceropath.org) (and specially the drivers and the students) for sample collection, in particular H. Vibol, K. Aun, K. Blasdell, and P. Buchy in Cambodia, K. Chaisiri in Thailand, and Kone in Lao PDR. We are indebted to S. Morand, M. Pagès, J. Claude, and J. Michaux as the coordinators of the CERoPath project (French ANR Biodiversity, grant ANR 07 BDIV 012) and the BiodivHealthSEA project (www.biodivhealthsea.org) (French ANR CP&ES, grant ANR 11 CPEL 002). Access to the “Plateforme ADN dégradé” (ISEM, UM) was provided by C. Tougard. Logistical support was also provided by Laboratorio de Ecología Molecular, Estación Biológica de Doñana, CSIC (LEM-EBD). We thank the State Ministry of Research and Technology (RISTEK, permit number: 028/SIP/FRP/SMII/2012) and the Ministry of Forestry, Republic of Indonesia for providing permits to carry out fieldwork in Indonesia. Likewise, we thank the Research Center for Biology, Indonesian Institute of Sciences (RCB-LIPI) and the MZB for providing staff and support to carry out fieldwork in the Moluccas. We also thank Sabah Parks (permits: TS/PTD/5/4 Jld. 45 (33) and TS/PTD/5/4 Jld. 47 (25)) for research permits and various kind of support, the Economic Planning Unit (reference: 100-24/1/299), and export permits from the Sabah Wildlife Department (JHL.600-3/7 Jld.7/19 and JHL.600-3/7 Jld.8/) and Sabah Biodiversity Council (reference: TK/PP:8/8Jld.2). This research received support from the SYNTHESYS project (<http://www.synthesys.info/>) which is financed by the European Community Research Infrastructure Action under the FP7 Integrating Activities Program (SYNTHESYS ACCESS GB-TAF-2735, GB-TAF-5026, and GB-TAF-5737 granted to PHF to the NHM, London; NL-TAF-5588 granted to MCS to the NBC, Leiden). The Spanish Ministry of Science and Innovation grants CGL2010-21524 and CGL2014-58793-P also supported this work. MCS is supported by the Spanish Ministry of Science and Innovation Predoctoral Fellowship BES-2011-049186. PHF was funded by a Marie-Curie fellowship (PIOF-GA-2012-330582-CANARIP-RAT). This publication is contribution No. 2017-123 SUD of the Institut des Sciences de l'Evolution de Montpellier (UMR 5554-CNRS-IRD).

SUPPLEMENTARY DATA

Supplementary data are available at *Journal of Mammalogy* online.

Supplementary Data SD1.—Supplementary methods.

Supplementary Data SD2.—PhyloBayes reconstructions for protein-coding genes from mitogenomes, *rag1*, *rbp3*, and *ghr*.

Supplementary Data SD3.—Eigen values for each axis of the skull comparison between *Sundamys* and *Rattus*.

Supplementary Data SD4.—Loading values for each axis of the skull comparison between *Sundamys* and *Rattus*.

Supplementary Data SD5.—Eigen values for each axis of the cranium comparison among *Sundamys* species.

Supplementary Data SD6.—Loading values for each axis of the cranium comparison among *Sundamys* species.

Supplementary Data SD7.—Eigen values for each axis of the dentary comparison among 585 *Sundamys* species.

Supplementary Data SD8.—Loading values for each axis of the dentary comparison among 585 *Sundamys* species.

LITERATURE CITED

ACHMADI, A. A. S., J. A. ESSELSTYN, K. C. ROWE, I. MARYANTO, AND M. T. M. ABDULLAH. 2013. Phylogeny, diversity, and biogeography

- of Southeast Asian spiny rats (*Maxomys*). *Journal of Mammalogy* 94:1412–1423.
- ADAMS, D. C., AND E. OTÁROLA-CASTILLO. 2013. geomorph: an R package for the collection and analysis of geometric morphometric shape data. *Methods in Ecology and Evolution* 4:393–399.
- APLIN, K. P., ET AL. 2011. Multiple geographic origins of commensalism and complex dispersal history of black rats. *PLoS One* 6:e26357.
- BENTON, M. J., AND P. C. J. DONOGHUE. 2007. Paleontological evidence to date the tree of life. *Molecular Biology and Evolution* 24:26–53.
- BONHOTE, J. L. 1903. Report on the mammals. *Fasciculi Malayenses* 1:30–31.
- BOOKSTEIN, F. L. 1991. *Morphometric tools for landmark data: geometry and biology*. Cambridge University Press, New York.
- BOROWIEC, M. L. 2016. AMAS: a fast tool for alignment manipulation and computing of summary statistics. *PeerJ* 4:e1660.
- BOUCKAERT, R., ET AL. 2014. BEAST 2: a software platform for Bayesian evolutionary analysis. *PLoS Computational Biology* 10:e1003537.
- CHAN, K. L. 1977. Enzyme polymorphism in Malayan rats of the Subgenus *Rattus*. *Biochemical Systematics and Ecology* 5:161–168.
- CHAN, K. L., S. S. DHALIWAL, AND H. S. YONG. 1979. Protein variation and systematics of three subgenera of Malayan rats (Rodentia: Muridae, genus *Rattus* Fischer). *Comparative Biochemistry & Physiology* 64:329–337.
- CHEN, W., Z. SUN, Y. LIU, B. YUE, AND S. LIU. 2012. The complete mitochondrial genome of the large white-bellied rat, *Niviventer excelsior* (Rodentia: Muridae). *Mitochondrial DNA* 23:363–365.
- CLAUDE, J. 2013. Log-shape ratios, Procrustes superimposition, elliptic Fourier analysis: three worked examples in *R*. *Hystrix* 24:94–102.
- CRANBROOK, E. OF, AHMAD, A. H. AND I. MARYANTO, 2014. The mountain giant rat of Borneo *Sundamys infraluteus* (Thomas) and its relations. *Journal of Tropical Biology and Conservation* 11:49–62.
- DRYDEN, I. L., AND K. V. MARDIA. 1998. *Statistical shape analysis*. Wiley, Chichester, United Kingdom.
- DEMOS, T. C., ET AL. 2016. Local endemism and within-island diversification of shrews illustrate the importance of speciation in building Sundaland mammal diversity. *Molecular Ecology* 25:5158–5173.
- DEN TEX, R.-J., R. THORINGTON, J. E. MALDONADO, AND J. A. LEONARD. 2010. Speciation dynamics in the SE Asian tropics: putting a time perspective on the phylogeny and biogeography of Sundaland tree squirrels, *Sundasciurus*. *Molecular Phylogenetics and Evolution* 55:711–720.
- ESSELSTYN, J. A., MAHARADATUNKAMSI, A. S. ACHMADI, C. D. SILER, AND B. J. EVANS. 2013. Carving out turf in a biodiversity hotspot: multiple, previously unrecognized shrew species co-occur on Java Island, Indonesia. *Molecular Ecology* 22:4972–4987.
- FABRE, P., ET AL. 2013. A new genus of rodent from Wallacea (Rodentia: Muridae: Murinae: Rattini), and its implication for biogeography and Indo-Pacific Rattini systematics. *Zoological Journal of the Linnean Society* 169:408–447.
- FABRE, P. H., ET AL. 2014. Rodents of the Caribbean: origin and diversification of hutias unravelled by next-generation museumics. *Biology Letters* 10:20140266.
- FABRE, P.-H., ET AL. 2016. Mitogenomic phylogeny, diversification, and biogeography of South American spiny rats. *Molecular Biology and Evolution* 34:613–633.
- HARRISON, J. 1955. The natural food of some rats and other mammals. *Bulletin of Raffles Museum* 25:157–165.
- HARRISON, J. L., AND B. L. LIM. 1950. Notes on some small mammals of Malaya. *Bulletin of Raffles Museum* 23:300–309.
- HARVEY, P. H., T. H. CLUTTON-BROCK, AND G. M. MACE. 1980. Brain size and ecology in small mammals and primates. *Proceedings of the National Academy of Sciences of the United States of America* 77:4387–4389.
- HAWKINS, M. T. R., K. M. HELGEN, J. E. MALDONADO, L. L. ROCKWOOD, M. T. N. TSUCHIYA, AND J. A. LEONARD. 2016. Phylogeny, biogeography and systematic revision of plain long-nosed squirrels (genus *Dremomys*, Nannosciurinae). *Molecular Phylogenetics and Evolution* 94:752–764.
- HEANEY, L. R., D. S. BALETE, E. A. RICKART, M. J. VELUZ, AND S. A. JANSA. 2009. Chapter 7. A new genus and species of small “tree-mouse” (Rodentia, Muridae) related to the Philippine giant cloud rats. *Bulletin of the American Museum of Natural History* 331:205–229.
- HUCHON, D., ET AL. 2002. Rodent phylogeny and a timescale for the evolution of glires: evidence from an extensive taxon sampling using three nuclear genes. *Molecular Biology and Evolution* 19:1053–1065.
- IUCN. 2015. The IUCN Red List of threatened species. Ver. 2015.3. www.iucnredlist.org. Accessed 16 December 2015.
- JANSA, S. A., F. K. BARKER, AND L. R. HEANEY. 2006. The pattern and timing of diversification of Philippine endemic rodents: evidence from mitochondrial and nuclear gene sequences. *Systematic Biology* 55:73–88.
- JANSA, S. A., AND M. WEKSLER. 2004. Phylogeny of muroid rodents: relationships within and among major lineages as determined by IRBP gene sequences. *Molecular Phylogenetics and Evolution* 31:256–276.
- JENTINK, F. A. 1879. On some hitherto undescribed species of *Mus* in the Leyden Museum. *Notes from the Leyden Museum* 2:13–19.
- JING, J., X. SONG, C. YAN, T. LU, X. ZHANG, AND B. YUE. 2015. Phylogenetic analyses of the harvest mouse, *Micromys minutus* (Rodentia: Muridae) based on the complete mitogenome sequences. *Biochemical Systematics and Ecology* 62:121–127.
- KATOH, K., K. MISAWA, K. KUMA, AND T. MIYATA. 2002. MAFFT: a novel method for rapid multiple sequence alignment based on fast Fourier transform. *Nucleic Acids Research* 30:3059–3066.
- KEARSE, M., ET AL. 2012. Geneious Basic: an integrated and extendable desktop software platform for the organization and analysis of sequence data. *Bioinformatics* 28:1647–1649.
- KIMURA, Y., M. T. R. HAWKINS, M. M. MCDONOUGH, L. L. JACOBS, AND L. J. FLYNN. 2015. Corrected placement of *Mus* - *Rattus* fossil calibration forces precision in the molecular tree of rodents. *Scientific Reports* 5:14444.
- KLOSS, C. B. 1908. New mammals from the Malay Peninsula. *Journal of the Federated Malay States Museum* 2:143–147.
- KOTLER, B. P., AND J. S. BROWN. 1988. Environmental heterogeneity and coexistence of desert rodents. *Annual Review of Ecology and Systematics* 19:281–307.
- LANFEAR, R., P. B. FRANDSEN, A. M. WRIGHT, T. SENFELD AND B. CALCOTT. 2016. PartitionFinder 2: new methods for selecting partitioned models of evolution for molecular and morphological phylogenetic analyses. *Molecular Biology and Evolution* 34:772–773.
- LARTILLOT, N., T. LEPAGE, AND S. BLANQUART. 2009. PhyloBayes 3: a Bayesian software package for phylogenetic reconstruction and molecular dating. *Bioinformatics* 25:2286–2288.
- LECOMTE, E., K. APLIN, C. DENYS, F. CATZEFLIS, M. CHADES AND P. CHEVRET. 2008. Phylogeny and biogeography of African Murinae based on mitochondrial and nuclear gene sequences, with

- a new tribal classification of the subfamily. *BMC Evolutionary Biology* 8:199.
- LEONARD, J. A., R. J. DEN TEX, M. T. R. HAWKINS, V. MUÑOZ-FUENTES, R. THORINGTON, AND J. E. MALDONADO. 2015. Phylogeography of vertebrates on the Sunda Shelf: a multi-species comparison. *Journal of Biogeography* 42:871–879.
- LI, H., ET AL. 2009. The Sequence Alignment/Map format and SAMtools. *Bioinformatics* 25:2078–2079.
- LIM, B.-L. 1966. Land molluscs as food of Malayan rodents and insectivores. *Journal of Zoology* 148:554–560.
- LIM, B.-L. 1970. Distribution, relative abundance, food habits, and parasite patterns of giant rats (*Rattus*) in West Malaysia. *Journal of Mammalogy* 51:730–740.
- LYON, M. W. 1908. Mammals collected in eastern Sumatra by Dr. W. L. Abbott during 1903, 1906, and 1907, with descriptions of new species and subspecies. *Proceedings of the United States National Museum* 34:619–679.
- MACE, G. M., P. H. HARVEY, AND T. H. CLUTTON-BROCK. 1981. Brain size and ecology in small mammals. *Journal of Zoology* 193:333–354.
- MARICIC, T., M. WHITTEN, AND S. PÄÄBO. 2010. Multiplexed DNA sequence capture of mitochondrial genomes using PCR products. *PLoS One* 5:e14004.
- MARTIN, M. 2011. Cutadapt removes adapter sequences from high-throughput sequencing reads. *EMBnet journal* 17:10–12.
- McCOMISH, B. J. 2012. Exploring biological sequence space: selected problems in sequence analysis and phylogenetics. Ph.D. dissertation, Massey University, New Zealand.
- MICHAUX, J., P. CHEVRET, AND S. RENAUD. 2007. Morphological diversity of Old World rats and mice (Rodentia, Muridae) mandible in relation with phylogeny and adaptation. *Journal of Zoological Systematics and Evolutionary Research* 45:263–279.
- MILLER, M. A., W. PFEIFFER, AND T. SCHWARTZ. 2010. Creating the CIPRES Science Gateway for inference of large phylogenetic trees. *Proceedings of the Gateway Computing Environments Workshop (GCE)*, 14 November 2010, New Orleans, Louisiana:1–8.
- MORRISON, D. A. 2008. How to summarize estimates of ancestral divergence times. *Evolutionary Bioinformatics* 2008:75–95.
- MUSSER, G. G. 1981. Results of the Archbold Expeditions. No. 105. Notes on systematics of Indo-Malayan murid rodents, and descriptions of new genera and species from Ceylon, Sulawesi, and the Philippines. *Bulletin of American Museum of Natural History* 168:229–334.
- MUSSER, G. G. 1986. Sundaic *Rattus*: definitions of *Rattus baluensis* and *Rattus korinchi*. *American Museum Novitates* 2862:1–24.
- MUSSER, G. G., AND M. D. CARLETON. 2005. Superfamily Muroidea. Pp. 894–1531 in *Mammal species of the World: a taxonomic and geographic reference* (D. E. Wilson and D. M. Reeder, eds.). 3rd ed. Johns Hopkins University Press, Baltimore, Maryland.
- MUSSER, G. G., AND C. NEWCOMB. 1983. Malaysian murids and the giant rat from Sumatra. *Bulletin of the American Museum of Natural History* 174:327–598.
- MUUL, I., AND L. B. LIAT. 1971. New locality records for some mammals of West Malaysia. *Journal of Mammalogy* 52:430–437.
- NILSSON, M. A., A. GULLBERG, A. E. SPOTORNO, U. ARNASON, AND A. JANKE. 2003. Radiation of extant marsupials after the K/T boundary: evidence from complete mitochondrial genomes. *Journal of Molecular Evolution* 57:3–12.
- PAGÈS, M., ET AL. 2010. Revisiting the taxonomy of the Rattini tribe: a phylogeny-based delimitation of species boundaries. *BMC Evolutionary Biology* 10:184.
- PAGÈS, M., ET AL. 2013. Cytonuclear discordance among Southeast Asian black rats (*Rattus rattus* complex). *Molecular Ecology* 22:1019–1034.
- PAGÈS, M., ET AL. 2015. Molecular phylogeny of South-East Asian arboreal murine rodents. *Zoologica Scripta* 45:349–364.
- PARADIS, E., J. CLAUDE, AND K. STRIMMER. 2004. APE: Analyses of phylogenetics and evolution in R language. *Bioinformatics* 20:289–290.
- PISANO, J., ET AL. 2015. Out of Himalaya: the impact of past Asian environmental changes on the evolutionary and biogeographical history of *Dipodoidea* (Rodentia). *Journal of Biogeography* 42:856–870.
- RENAUD, S., P. CHEVRET, AND J. MICHAUX. 2007. Morphological vs. molecular evolution: ecology and phylogeny both shape the mandible of rodents. *Zoologica Scripta* 36:525–535.
- ROBERTS, T. E., H. C. LANIER, E. J. SARGIS, AND L. E. OLSON. 2011. Molecular phylogeny of treeshrews (Mammalia: Scandentia) and the timescale of diversification in Southeast Asia. *Molecular Phylogenetics and Evolution* 60:358–372.
- ROBINS, J. H., P. A. McLENACHAN, M. J. PHILLIPS, L. CRAIG, H. A. ROSS, AND E. MATISOO-SMITH. 2008. Dating of divergences within the *Rattus* genus phylogeny using whole mitochondrial genomes. *Molecular Phylogenetics and Evolution* 49:460–466.
- ROBINS, J. H., P. A. McLENACHAN, M. J. PHILLIPS, B. J. McCOMISH, E. MATISOO-SMITH, AND H. A. ROSS. 2010. Evolutionary relationships and divergence times among the native rats of Australia. *BMC Evolutionary Biology* 10:375.
- ROHLF, F. 2013. tpsDIG2: digitize landmarks & outlines from image files, scanner, or video. <http://ife.bio.sunysb.edu/morph/soft-data-acq.html>. Accessed 2015.
- ROHLF, F., AND D. SLICE. 1990. Extensions of the Procrustes method for the optimal superimposition of landmarks. *Systematic Biology* 39:40–59.
- ROWE, K. C., K. P. APLIN, P. R. BAVERSTOCK, AND C. MORITZ. 2011. Recent and rapid speciation with limited morphological disparity in the genus *Rattus*. *Systematic Biology* 60:188–203.
- ROWE, K. C., M. L. RENO, D. M. RICHMOND, R. M. ADKINS, AND S. J. STEPPAN. 2008. Pliocene colonization and adaptive radiations in Australia and New Guinea (Sahul): multilocus systematics of the old endemic rodents (Muroidea: Murinae). *Molecular Phylogenetics and Evolution* 47:84–101.
- RUDD, R. L. 1965. Weight and growth in Malaysian rain forest mammals. *Journal of Mammalogy* 46:588–594.
- RUEDI, M., AND L. FUMAGALLI. 1996. Genetic structure of gymnures (genus *Hylomys*; Erinaceidae) on continental islands of Southeast Asia: historical effects of fragmentation. *Journal of Zoological Systematics and Evolutionary Research* 34:153–162.
- SAMUELS, J. X. 2009. Cranial morphology and dietary habits of rodents. *Zoological Journal of the Linnean Society* 156:864–888.
- SATOH, K. 1997. Comparative functional morphology of mandibular forward movement during mastication of two murid rodents, *Apodemus speciosus* (Murinae) and *Clethrionomys rufocanus* (Arvicolinae). *Journal of Morphology* 231:131–141.
- SCHENK, J. J., K. C. ROWE, AND S. J. STEPPAN. 2013. Ecological opportunity and incumbency in the diversification of repeated continental colonizations by muroid rodents. *Systematic Biology* 62:837–864.
- SEN, Y. H. 1969. Karyotypes of Malayan rats (Rodentia-Muridae, genus *Rattus* Fischer). *Chromosoma* 27:245–267.
- SHARIFF, S. M. 1990. Ectoparasites of small mammals trapped at the Ulu Gombak Forest, Selangor Darul Ehsan. *The Journal of the Wildlife and Parks* IX:9–17.

- SIKES, R. S., AND THE ANIMAL CARE AND USE COMMITTEE OF THE AMERICAN SOCIETY OF MAMMALOGISTS. 2016. 2016 Guidelines of the American Society of Mammalogists for the use of wild mammals in research and education. *Journal of Mammalogy* 97:663–688.
- SLICE, D. E. 2007. Geometric Morphometrics. *Annual Review of Anthropology* 36:261–281.
- STEPHAN, S., R. ADKINS, AND J. ANDERSON. 2004. Phylogeny and divergence-date estimates of rapid radiations in muroid rodents based on multiple nuclear genes. *Systematic Biology* 53:533–553.
- STEPHAN, S. J., R. M. ADKINS, P. Q. SPINKS, AND C. HALE. 2005. Multigene phylogeny of the Old World mice, Murinae, reveals distinct geographic lineages and the declining utility of mitochondrial genes compared to nuclear genes. *Molecular Phylogenetics and Evolution* 37:370–388.
- TAMURA, K., G. STECHER, D. PETERSON, A. FILIPSKI, AND S. KUMAR. 2013. MEGA6: Molecular evolutionary genetics analysis version 6.0. *Molecular Biology and Evolution* 30:2725–2729.
- TILAK, M. K., F. JUSTY, M. DEBIAIS-THIBAUD, F. BOTERO-CASTRO, F. DELSUC, AND E. J. P. DOUZERY. 2015. A cost-effective straightforward protocol for shotgun Illumina libraries designed to assemble complete mitogenomes from non-model species. *Conservation Genetics Resources* 7:37–40.
- TSANGARAS, K., ET AL. 2014. Hybridization capture using short PCR products enriches small genomes by capturing flanking sequences (CapFlank). *PLoS One* 9:e109101.
- WANG, S., H. CONG, L. KONG, M. MOTOKAWA, AND Y. LI. 2015. Complete mitochondrial genome of the greater bandicoot rat *Bandicota indica* (Rodentia: Muridae). *Mitochondrial DNA* 1736:1–2.
- WELLS, K., E. K. V. KALKO, M. B. LAKIM, AND M. PFEIFFER. 2007. Effects of rain forest logging on species richness and assemblage composition of small mammals in Southeast Asia. *Journal of Biogeography* 34:1087–1099.
- WILSON, D. E., K. M. HELGEN, C. S. YUN, AND B. GIMAN. 2006. Small mammal survey at two sites in planted forest zone, Bintulu, Sarawak. *Malayan Nature Journal* 59:165–187.
- YOSIDA, T. H. 1973. Evolution of karyotypes and differentiation in 13 *Rattus* species. *Chromosoma* 40:285–297.
- 478137, 478139, 478145–46, 478149. Males: AMNH 102547; BMNH 9.4.1.441, 55.2910, 55.2913, 55.2917, 55.939, 55.946; DMNH 6196; FMNH 63154–55, 63157; MNHN CG1977N211, CG1981N258, CG1981N256, CG1990N573; RMNH 18351; USNM 113035, 113052, 114290, 478127, 478129, 478131, 478125. *Sundamys annandalei*. Females: BMNH 553152, 553156; MNHN CG1980N224, CG1981N246, CG1981N248, CG1981N250, CG1981N235–7. Males: BMNH 553153–55; MNHN CG1980N223, CG1980N241, CG1981N233–4, CG1981N238–9, CG1981N242, CG1981N249, CG1981N251, CG1981N254, CG1981N255; MZB 28969. *Rattus baluensis*. Females: FMNH 108908–9, 108911, 108915, 108924; USNM 292696, 292698. Males: BMNH 712771; MZB 5633. *Rattus andamanensis*. Females: USNM 111852, 238174, 279261, 533731, 564485. Males: USNM 111837, 533435–6, 533732–3. *Rattus argentiventer*. Females: MNHN CG1924N281, CG1924N285, CG1969N151. Males: MNHN CG1929N274, CG1957N547, CG1971N808, CG1977N232, CG1977N234, CG1982N101–2. *Rattus exulans*. Females: CBGP L219, L256, K52–53, K62. Males: CBGP L271, K63, K58, K61, R4094. *Rattus losea*. Females: CBGP L268, R4250, R5062, R5190; RMNH 22657. Males: AMNH 275553; CBGP R4791, R4857, R5195; RMNH 22656. *Rattus norvegicus*. Females: CBGP 2446812. Males: CBGP 2446813. *Rattus rattus*. Females: RMNH 9802, 9814. Males: CBGP R121, R129, R132, R148, R149, R152–3; ZMUC 13694. *Rattus tanezumi*. Females: CBGP L8, R4271, R5189, R5422, R5433. Males: CBGP L50, R4114, R4878, R4997; MZB 22715. *Rattus tiomanicus*. Females: USNM 197476–80. Males: MZB 34436; USNM 197481, 197483, 197484.

APPENDIX II

SPECIMENS USED FOR THE DENTARY LATERAL SIDE IN THE MORPHOMETRIC GEOMETRIC ANALYSIS

Sundamys infraluteus. Females: BMNH 712840, 712842, 712844; FMNH 108934, 108936; MCZ 36107; MZB 5084, 23609; RMNH 21253; USNM 292759, 292764, 292766–8, 292770, 301076. Males: BMNH 712839, 712841; FMNH 108932–33, 108935, 108937; MCZ 36105–6, 36108; USNM 292765, 301075, 301077. *Sundamys maxi*. Females: RMNH 13566, 13576, 14206–7, 14209, 21479. Males: RMNH 13968, 14181, 14205, 14210–1. *Sundamys muelleri*. Females AMNH 103606–7, 103762–4, 103766, 103768–9; BMNH 552911, 552914, 552918, 552920, 55944–5; MNHN CG1981N259, CG1981N260, CG1990N572; USNM 114286–9, 114291, 114378, 114380, 114382, 478128, 478130, 478137, 478139, 478145. *Sundamys annandalei*. Females: BMNH 32.516, 553157, 553159–60; MNHN CG1980N224, CG1981N235–7, CG1981N246, CG1981N248, CG1981N250. Males: BMNH 50.952–3, 553158, 611217; MNHN CG1980N241, CG1981N233, CG1981N238–9, CG1981N247, CG1981N249, CG1981N251, CG1981N254–5; MZB 28969.

APPENDIX I

SPECIMENS USED FOR THE PALATAL VIEW OF THE SKULL IN GEOMETRIC MORPHOMETRIC ANALYSIS

Sundamys infraluteus. Females: BMNH 71.2840, 71.2842, 71.2844; MCZ 36107; MZB 23609; FMNH 108934, 108936; USNM 292759, 292763–4, 292766–8, 292770, 301076. Males: AMNH 106669; BMNH 71.2839, 71.2841; FMNH 108932–3, 108935, 108937; MCZ 36105–6, 36108; USNM 292765, 301075, 301077. *Sundamys maxi*. Females: RMNH 14207, 21479. Males: RMNH 14181, 14205–06, 14210–11, 13566. *Sundamys muelleri*. Females: AMNH 102804–5, 103606; BMNH 9.4.1.437–38, 55.2911, 55.2914, 55.2918, 55.2920; RMNH 21469, 21470, 23279; USNM 104838–39, 113036, 113039, 114286, 114620, 114622, 115585, 115587, 478119, 478121–2, 478128, 478130,

Submitted 19 September 2016. Accepted 13 June 2017.

Associate Editor was Jake Esselstyn.